

Figure 1. Schematic Drawing of the Test Apparatus.

Table 1 gives the chemical composition, percentage and flow rate of each composition in the sampled gases. As is evident, each sample contained  $H_2$ ,  $CH_4$ ,  $H_2O$ ,  $N_2$ ,  $CO$ ,  $O_2$ ,  $Ar$ , and  $CO_2$ . Limestone concrete contains 43% by wt  $H_2O$  and  $CO_2$ , which are released at elevated temperatures.  $H_2$  results from  $H_2O$  dissociation.  $CH_4$  and  $CO$  result from reaction of  $H_2$  and  $CO_2$  with very hot graphite. Furthermore, reaction of water vapor with graphite, dissociation of  $CO_2$ , as well as reaction of  $UO_2$  with calcite could contribute to a high volume % of  $CO$ .  $N_2$  and some of the  $O_2$  could be the excess air left in the system and  $Ar$  is the purged gas. Volume % of different gases in each sample is dependent on the concrete temperature at the time the sample was taken. As expected, rates of water vapor and  $H_2$  in the first sample is large. The small amount of  $CO$  and  $CO_2$  is due to reaction of  $H_2O$  vapor with graphite. In the second sample,  $H_2$  has decreased but  $CO$  and  $CO_2$  has increased.  $H_2$  in the third sample, for all practical reasons, has approached zero whereas  $CO$  has attained maximum value. Nevertheless, the type of chemical composition that comprises any sample beyond  $1200^\circ C$  resembles the result of sample #3 until the experiment is terminated. In relation to reactor technology, once the initial heating phase of concrete is overcome, presence of  $H_2$  is expected to be minute. However, considerable amounts of  $CO$  and  $CO_2$  can be present in the containment building which can safely enter into the atmosphere, in the event the breach of the containment building is encountered.

The aerosol sampling device did not show any detectable radioactive particles. In the process of melting, penetration and gas release, the gases did not carry any  $UO_2$  particles. The detectable aerosol particles were mostly  $C$  and very minute concrete constituents.

Radial expansion measurements of concrete by the displacement transducer is given in Fig. 2 in terms of time, and in Fig. 3 in

Table 1. Analyzed Sampled Gases and Their Respective Rates

Samples	H <sub>2</sub> % Vol. (cc/min)	CH <sub>4</sub> % Vol. (cc/min)	H <sub>2</sub> O % Vol. (cc/min)	CO % Vol. (cc/min)	CO <sub>2</sub> % Vol. (cc/min)	N <sub>2</sub> % Vol. (cc/min)	O <sub>2</sub> % Vol. (cc/min)	Ar % Vol. (cc/min)
#1	82. (713.4)	.3 (2.61)	.5 (4.35)	3.9 (33.93)	3.1 (26.97)	1.7 (14.79)	.3 (2.61)	8.2 (71.34)
#2	26.5 (429.3)	.2 (3.24)	.6 (9.72)	28.1 (455.22)	21.9 (354.78)	7.9 (127.98)	2.0 (32.4)	12.8 (207.36)
#3	.4 (20.4)	< .02 ( < 1.02)	.4 (20.4)	83.2 (4243.2)	.7 (35.7)	9.0 (45.9)	2.4 (122.4)	3.9 (198.9)

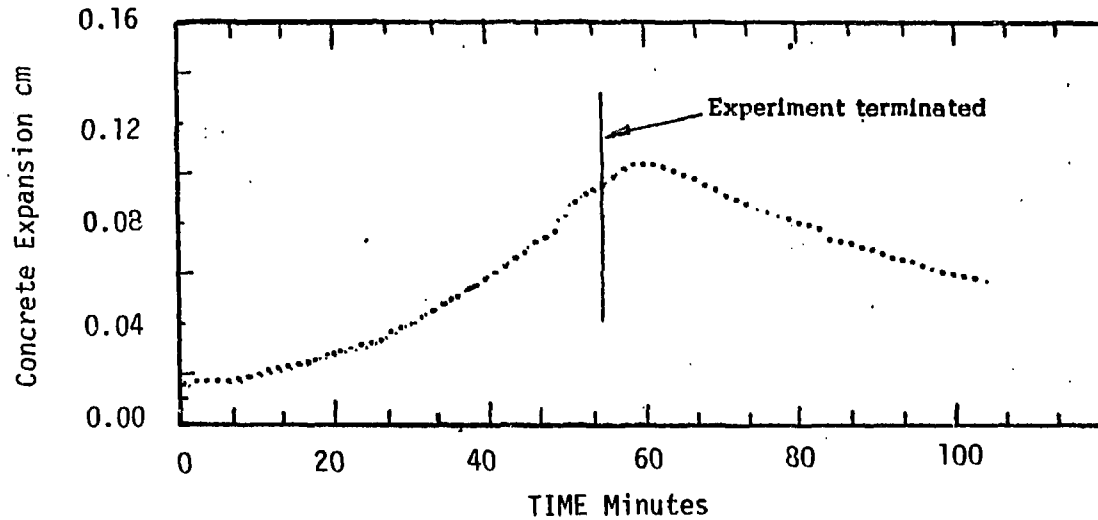


Figure 2. Concrete Expansion as a Function of Time.

terms of temperature. Radial expansion of concrete at the #6 thermocouple reaches a maximum of 0.087 cm about 5 minutes after the experiment is terminated. Referring to Fig. 3, it is evident that this maximum does not occur at the maximum temperature of 700°C. At the maximum temperature concrete has gone through slight compression, 0.054 cm. Accordingly, expansion of concrete can be attributed solely to pore pressure established by migrating water. Reversal in the expansion of concrete can be due to removal of the water from concrete and the drying of the concrete which in turn contributes to the relief of stresses caused by pore pressure. The failure time and distance of the two consecutive thermocouples is used in calculating the penetration rate of  $UO_2$  into concrete. This amounted to about .23 cm/min. Using radiograph of Fig. 4 and experimental time of 30 min similar rate is obtained. Furthermore, the radiograph clearly indicates the uniform downward heat transfer into concrete and relatively small heat loss in the radial direction, about 20%.

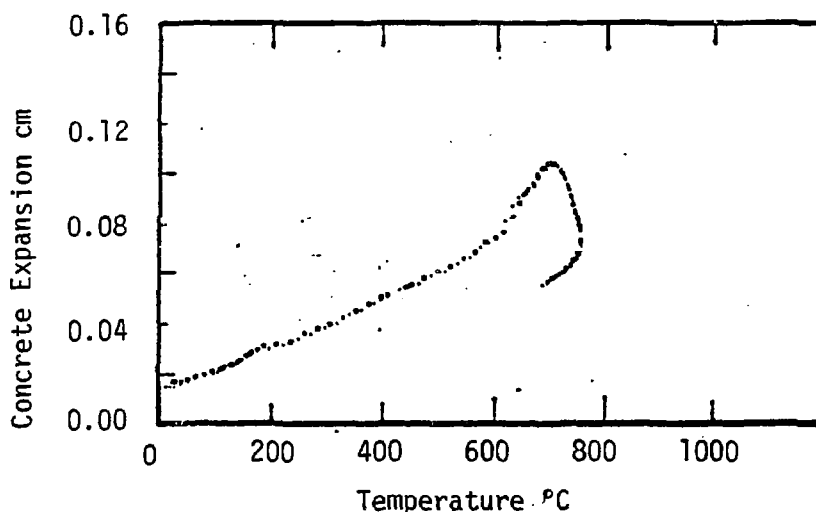


Figure 3. Concrete Expansion as a Function of Temperature.

Post-experimental analysis of the sample indicated more or less similar results as were described by Farhadieh and Gunther.<sup>1</sup> The solid mass of  $UO_2$ /concrete mixture, that resulted from the penetration of  $UO_2$  into concrete, had a porous, volcanic appearance and was relatively brittle. The top surface of the mass, looking into the overlying cavity, contained random holes 3-7 mm in diameter, which were indicative of gas release sites through the once-molten mixture (Fig. 5). It is likely that gas pockets were locally formed between the molten mass and top surface of the solid concrete which were removed by Rayleigh Taylor instability mechanism. Similar phenomenology was observed in melting of an immiscible system, but the melt film was continuous.

Electron probe analysis of selected  $UO_2$ /concrete samples showed more or less uniform distribution of  $UO_2$  and concrete constituents. X-ray analysis of similar samples indicated formation of  $CaU_2O_6$  and  $Ca_2U_2O_7$  chemical compounds between  $UO_2$  and concrete constituents.

Inspection of the post-experimental concrete samples indicated presence of about 5-mm-thick white powder, mostly CaO, at the interface of concrete and UO<sub>2</sub>/concrete solidified mass. The underlying concrete mass, though not decomposed, was heavily dehydrated. Inspection of the concrete sample two days later revealed that the dehydrated region of concrete, extending about 3 cm below the surface, had swollen considerably, with virtually no strength.

Plans are to include some typical fission particles in the experiments to study the airborne capability of the particles upon penetration, gas release, and aerosol formation, and to carry out similar experiments with basalt and magnetite type concrete for comparison with the limestone concrete. It should be mentioned that the first test on basalt concrete was successfully carried out.

#### References

1. R. Farhadieh and W. H. Gunther, "One-Dimensional Penetration of Molten UO<sub>2</sub> Into Substrate Limestone Concrete," Nuclear Tech., 50, 298 (1980).
2. L. Baker, Jr., "Characterization of Concrete," Reactor Development Program Progress Report, ANL-RDP-75, p. 6.3, Argonne National Laboratory (Sept. 1978).
3. T. Z. Harmathy, "Thermal Properties of Concrete at Elevated Temperatures," J. Mater., 5, 2, 47 (1970).

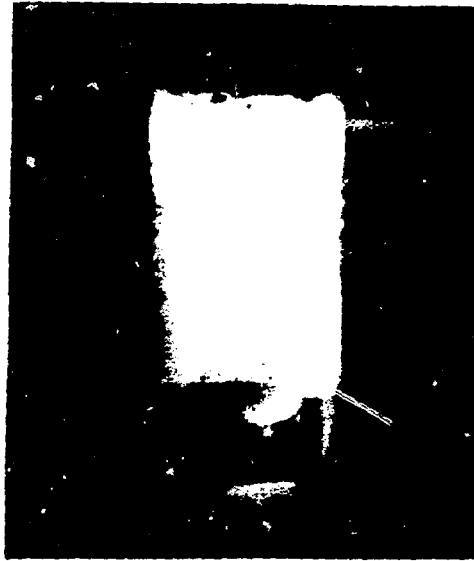


Figure 4. Posttest Radiograph of the Test Section Depicting  $UO_2$  Penetration into Concrete.



Figure 5. Posttest Photograph Surface of  $UO_2$ /Concrete Mixture Depicting the Gas Release Sites.

## **DISCLAIMER**

This report was prepared as an account of work sponsored by an agency of the United States Government. Neither the United States Government nor any agency thereof, nor any of their employees, makes any warranty, express or implied, or assumes any legal liability or responsibility for the accuracy, completeness, or usefulness of any information, apparatus, product, or process disclosed, or represents that its use would not infringe privately owned rights. Reference herein to any specific commercial product, process, or service by trade name, trademark, manufacturer, or otherwise does not necessarily constitute or imply its endorsement, recommendation, or favoring by the United States Government or any agency thereof. The views and opinions of authors expressed herein do not necessarily state or reflect those of the United States Government or any agency thereof.